08 Sep 1985

Vibration Coupling In Continuous Belt And Band Systems

C. D. Mote

W-Z Ben Wu

Missouri University of Science and Technology

Recommended Citation

C. D. Mote and W. B. Wu, "Vibration Coupling In Continuous Belt And Band Systems," *Journal of Sound and Vibration*, vol. 102, no. 1, pp. 1 - 9, Elsevier, Sep 1985.
The definitive version is available at https://doi.org/10.1016/S0022-460X(85)80099-7

Journal of Sound and Vibration (1985) **102**(1), 1-9

VIBRATION COUPLING IN CONTINUOUS BELT AND BAND SYSTEMS

C. D. MOTE JR.

Department of Mechanical Engineering, University of California, Berkeley, California 94720, *U.S.A.*

AND

W. Z. WU

Department of Engineering Mechanics, University of Missouri-Rolla, Rolla, Missouri 65401, *U.S.A.*

(*Received* 3 *September* 1983, *and in revised form* 2 *June* 1984)

Small transverse oscillation of an endless band supported by wheels couples the response of the free spans of the band to oscillation of the wheels. The coupling arises from the finite curvature of the free spans of the band when its bending stiffness is finite. Significant modeling error can occur if a single span of the band is modeled as a simply supported, axially moving beam. The coupling provides an opportunity to dissipate vibration energy. Experiments and finite element analyses support the coupling discussion presented.

1. INTRODUCTION

The natural frequencies of oscillation of high speed band saws and the stability of these band saws under the influence of in-plane forces have been extensively investigated over the past decade or so [1-12]. In the band saw models of these analyses the band is considered to be an axially moving beam or plate whose principal, or working, span is isolated from the remainder of the band saw system by either fluid film guide bearings or by the drive wheels themselves. The end conditions for the practical span of the band are modeled as simple supports, thereby explicitly decoupling the response of the principal span from the responses of the wheels and the remainder of the band outside the principal span. However, transverse vibration of an endless band loop couples response of the entire band to that of the wheels, rather than isolating oscillation of a segment of the band from the remainder of the system. Accordingly, the model for vibration of the principal span cannot be decoupled from the remainder of the system without some loss of model fidelity.

The mechanism of vibration coupling occurring in a continuous band saw - wheel system is discussed in what follows here. The coupling between the spans is shown to depend upon the initial curvature of the band spans between the wheels or guides: finite curvatures of the spans lead to coupling and vanishing curvatures lead to decoupling of the span motions from small transverse displacements of the band. Coupling between the vibration of the principal span and the vibration of the secondary, or return, span results in a propagation vibration energy between them. Because of this energy propagation, an opportunity exists for vibration control in the principal span of a band saw through dissipation of energy in the secondary span by active or passive means.

Experiments on a full-scale band mill demonstrated the coupling and the energy flux between spans. Analyses on a finite element model confirmed the laboratory observations and the explanation of the coupling mechanism presented here.

0022-460X/85/170001+09 $03.00/0

2. OBSERVED COUPLING PHENOMENON

The experimental apparatus used to examine the coupling phenomenon is schematically shown in Figure 1. The band was a commercial (Stenner) band saw with 0·9 m diameter wheels and an axle to axle wheel separation of 1·26 m. The toothless band plate had a rectangular cross section, $1 \times 66\ mm^2$. The band tension was approximately 700 N. The principal and secondary spans were identical for all intents and purposes. The drive motor was disconnected from the wheels to reduce dissipation during band vibration. Excitation of the band vibration was provided by an electromagnet during resonance tests and by an impact hammer during modal analyses. The transverse motion of each span was monitored with a single, reluctance type, displacement transducer.

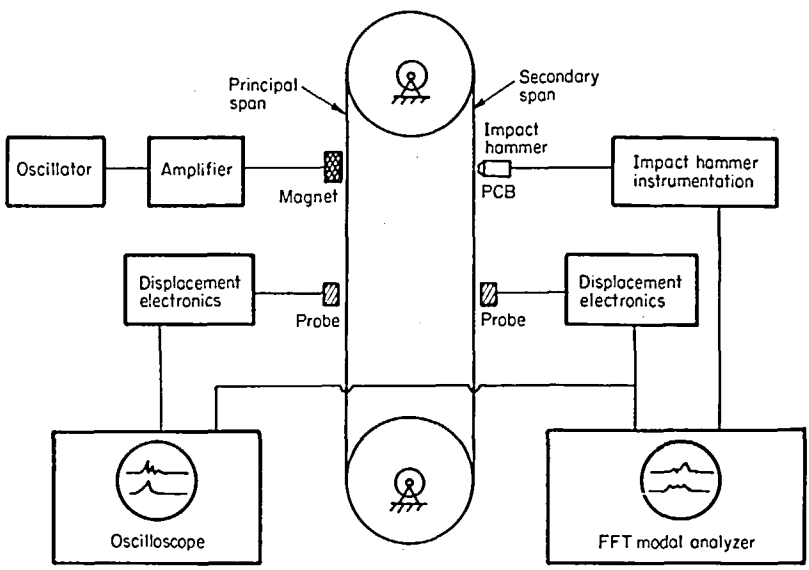

Figure 1. Schematic of the band model and the experiment.

Attention was directed to the isolation of the vibration in the principal and secondary spans by the wheels. A transverse disturbance of one span generated vibration displacement in the other (see Figure 2(a)). The phase difference between the vibration in the two spans was almost exactly 90 degrees. The vibration frequencies of the two spans were essentially identical. An expansion of the time scale of the transverse displacement record showed a characteristic low frequency modulation of a high frequency vibration, as shown in Figure 2(b). The modulated response demonstrates the coupling of the principal and secondary span vibrations, and it shows a propagation of energy between them. The auto spectra for the transverse vibration in the two spans, and the coherence and phase spectra of their mutual vibration, are shown in Figure 3. The phase spectrum in Figure 3(d) was measured with the probes located as shown in Figure 1. In-phase (out-of-phase) transverse displacement of the two spans at the displacement probes corresponds to a phase of +180° (0°) in Figure 3(d).

The beating oscillation in Figure 2(b) resulted from the two natural modes shown in Figure 3. The lower natural frequency in Figures 3(a) and (b), 13·5 Hz, is an in-phase vibration of the spans and the higher natural frequency, 14·5 Hz, is an out-of-phase mode. These modes are illustrated in Figures 4(a) and (b), respectively. The in-phase oscillation

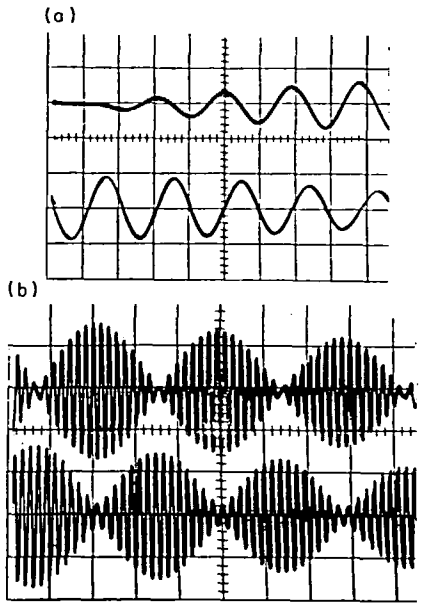

Figure 2. Transverse response for disturbance of the principal span. Upper trace, principal span; lower trace, secondary span. (a) Sweep rate, 50 ms/div; (b) sweep rate, 500 ms/div.

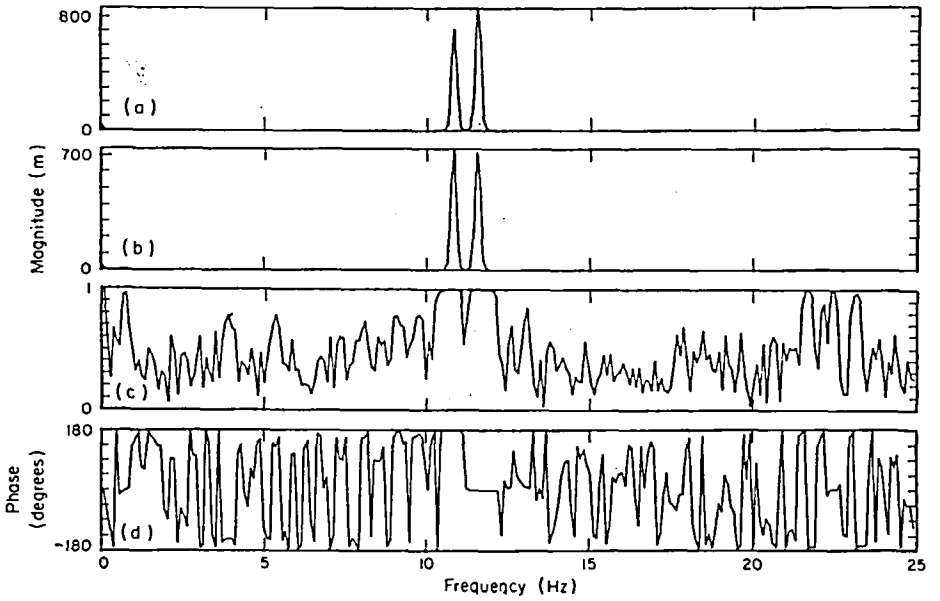

Figure 3. (a) Auto spectrum for the disturbed span; (b) auto spectrum for the undisturbed span; (c) coherence spectrum; (d) phase spectrum.

in Figure 4(a) requires angular acceleration of the wheels. The out-of-phase oscillation, Figure 4(b), does not accelerate the wheels.

The vibration observed in Figure 2 was a linear combination of the in-phase and out-of-phase modes:

$$Y_p = Y_1 + Y_2, \qquad Y_s = Y_1 - Y_2, \tag{1}$$

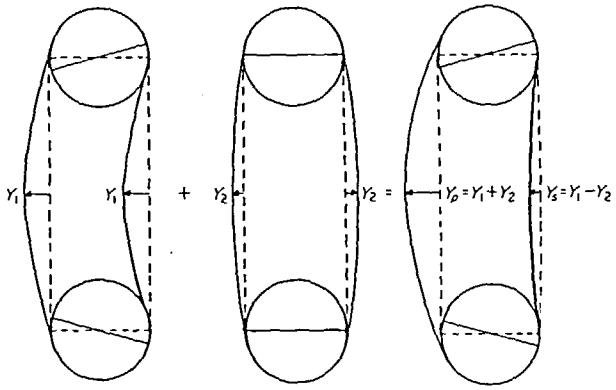

Figure 4. Combined response of the band in first two modes. (a) First in-phase mode; (b) first out-of-phase mode; (c) superimposed vibration.

where subscripts p and s refer to the principal and secondary spans, and the subscripts 1 and 2 refer to the in-phase and out-of-phase modes respectively (a list of symbols is given in the Appendix). For the initial conditions

$$Y_p(0, X) = 2a \sin(\pi X/l) = 2A(X), \qquad Y_s(0, X) = \partial Y_p(0, X)/\partial t = \partial Y_s(0, X)/\partial t = 0 \quad (2)$$

the response becomes

$$Y_p = 2A(X) \cos(\omega_{\text{mod}} t) \cos(\omega_{\text{ave}} t), \qquad Y_s = 2A(X) \sin(\omega_{\text{mod}} t) \sin(\omega_{\text{ave}} t), \quad (3)$$

where $\omega_{\text{ave}} = \frac{1}{2}(\omega_0 + \omega_i)$, $\omega_{\text{mod}} = \frac{1}{2}(\omega_0 - \omega_i)$ and ω_i and ω_0 are the natural frequencies of the in-phase and the out-of-phase modes, respectively. When $\omega_i \approx \omega_0$ so that $\omega_{\text{mod}} \ll \omega_{\text{ave}}$ the "beating" modulation observed in Figure 2(b) occurs.

The local maximum kinetic energy in the principal and secondary spans, occurring during any period $2\pi/\omega_{\text{ave}}$, can be represented by

$$E_p = \tfrac{1}{2} \int_0^l \rho \left(\frac{\partial Y_p}{\partial t} \right)^2 \mathrm{d}X \simeq \rho a^2 l \omega_{\text{ave}}^2 \cos^2(\omega_{\text{mod}} t),$$

$$E_s = \tfrac{1}{2} \int_0^l \rho \left(\frac{\partial Y_s}{\partial t} \right)^2 \mathrm{d}X \simeq \rho a^2 l \omega_{\text{ave}}^2 \sin^2(\omega_{\text{mod}} t), \quad (4)$$

where ρ is the mass of the band per unit length, and l is the length of each span. Equation (4) expresses the modulation of the maximum kinetic energy, $E = \rho a^2 l \omega_{\text{ave}}^2$, in each span. The local maximum kinetic energy in the spans can alternatively be described by

$$E_p = \tfrac{1}{2} E[1 + \cos(2\omega_{\text{mod}} t), \qquad E_s = \tfrac{1}{2} E[1 - \cos(2\omega_{\text{mod}} t), \quad (5)$$

showing the energy flux between the spans at frequency $2\omega_{\text{mod}}$.

The flux of energy between the spans provides the opportunity to dissipate vibration energy in the principal span by damping the secondary span. This is illustrated in the data of Figure 5. The principal span of the band was plucked and released from rest, producing the modulated vibration amplitude envelope shown in both spans. Light (unspecified) damping, applied to the secondary span at the time shown in Figure 5, dissipated the vibration energy in both spans.

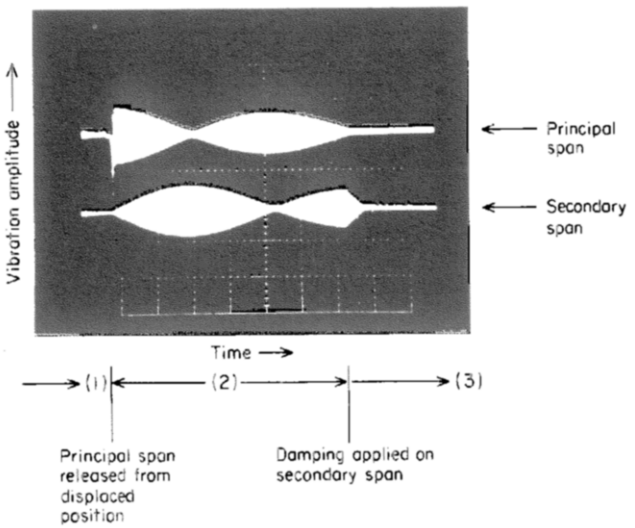

Figure 5. Disturbance of the principal span followed by light damping on the secondary span. (1), At rest; (2), free vibration; (3), damping applied.

3. MECHANISM OF COUPLING BETWEEN SPANS

Simultaneous spectral analyses of the rotation of a wheel and of the transverse vibration of the secondary span were computed while the principal span was harmonically excited with the electromagnet. At excitation frequency 13·5 Hz, corresponding to the lowest natural frequency and the in-phase mode, significant angular acceleration of the wheel occurred as shown in Figure 6(a). At excitation frequency 14·5 Hz, corresponding to the out-of-phase mode in Figure 6(b), the wheel angular acceleration was negligible. Small, in-phase, transverse displacements of the band spans rotated the wheels from the configuration denoted by dashes to that depicted by solid lines in Figure 4(a). Small, out-of-phase, transverse displacements of the spans of equal amplitude did not rotate the wheels.

The uniform band, when completely unloaded by the wheels, assumes the form of a circular hoop. When stretched by the wheels, the band becomes nearly, though not perfectly, a straight span between the wheels as schematically illustrated in Figure 7(a). Euler-Bernoulli theory applied to the band just in contact with the wheels requires

$$M = EI/R, \tag{6}$$

where R is the radius of curvature of the wheel, EI is the bending stiffness of the band and M is the bending moment in the band around the wheels. Equilibrium of the span segment in Figure 7(b) requires

$$M = Td/2, \tag{7}$$

where T is the band tension at midspan, and d is the offset of the band at the midspan from the tangent to the wheels. The offset d is estimated from equations (6) and (7) to be

$$d = 2EI/TR. \tag{8}$$

As $T \to \infty$, $d \to 0$ within Euler-Bernoulli theory.

The curvature of the band, resulting from its finite bending stiffness, is the key to the coupling phenomenon. The span length between wheel contact points exceeds the free path length along the mutual tangent to the wheels. Initial transverse deflection of a band

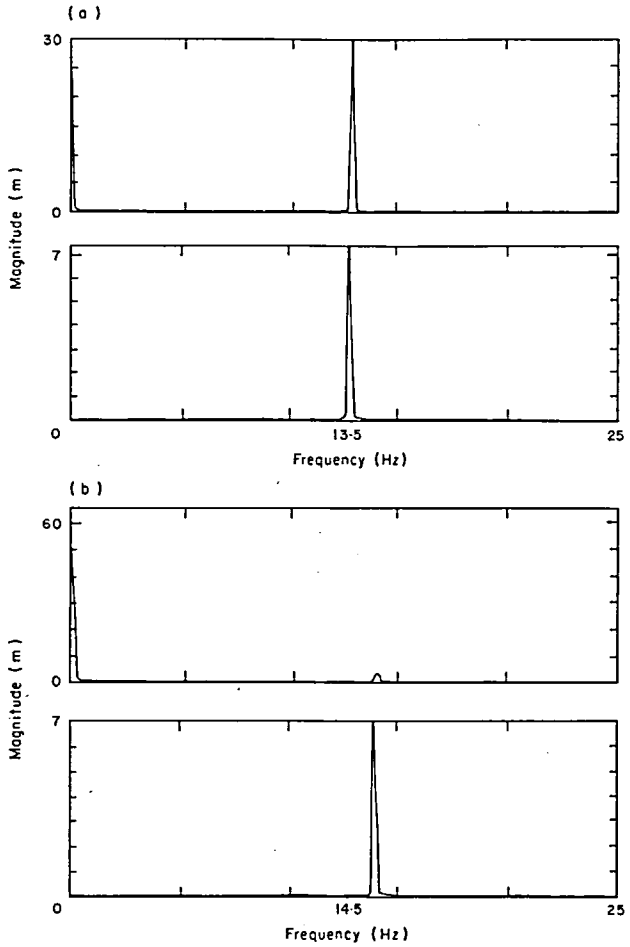

Figure 6. Spectral analyses of span transverse vibration and wheel rotation. Upper trace, auto spectrum of wheel rotation; lower trace, auto spectrum of span transverse vibration. (a) Lower resonant frequency; (b) higher resonant frequency.

span toward the centerline of the band-wheel system rotates the wheels to accommodate the "flattening" of the span onto the tangent line. The principal point is that the spans are not straight in the equilibrium configuration. When the band was replaced by a string with truly negligible bending stiffness, no vibration coupling was observed. When the band was cut into two strips each clamped to the wheels without bending them around the wheels, the coupling also disappeared. Small initial tension in the band results in stiffness-dominated restoring forces, relatively large initial curvature of the spans and accordingly increased coupling was expected and observed. Increasing tension results in a more "string-like" band and coupling decreased and disappeared for sufficiently large tension.

The natural modes of the band are simply degenerate in the event of equal span lengths and vanishing initial span curvature (vanishing bending around the wheels). The natural frequencies and mode shapes of one span are identically repeated in the other in this case. The introduction of small curvature introduces asymmetry in the mode and causes the repeated natural frequencies to split into two distinct natural frequencies. The lower frequency will always be associated with an angular acceleration of the wheels, and the

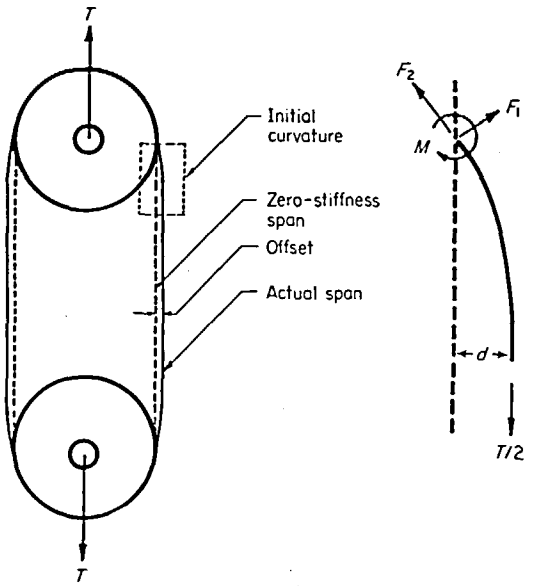

Figure 7. Initial curvature of the band.

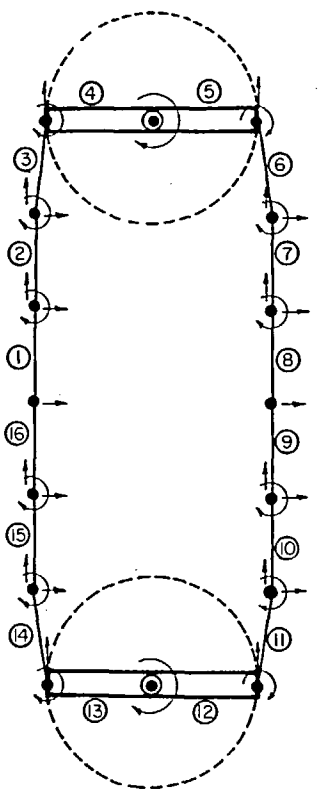

Figure 8. Finite element model for a band system.

higher one will not accelerate the wheels. Increasing band tension raises the natural frequencies and causes the two split natural frequencies to converge by reducing the equilibrium curvature of the spans. Decreasing band tension reduces natural frequencies and causes the split natural frequencies to further diverge.

A finite element model representing the band system as a finite assemblage of discrete beam elements is shown in Figure 8. The elements translate, rotate and bend in the plane. The initial band curvature was approximated by offsetting the span elements as shown in Figure 8. The natural modes of the band system were computed by using standard routines for different offsets. For small offsets, in-phase and out-of-phase vibration modes, virtually identical to those shown in Figures 4(a) and (b), were computed. For vanishing offsets, the degenerate case of uncoupled vibration modes in each span alone were computed.

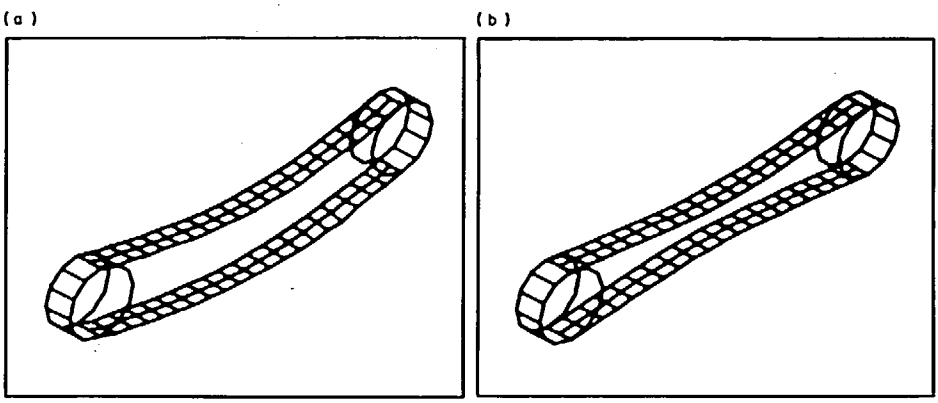

Figure 9. Experimental model analysis showing (a) In-phase and (b) out-of-phase modes.

Finally, a modal analysis was undertaken on the band mill with use of the impact hammer two-channel FFT analyzer technique. The transfer functions between the span transverse response and the impulse excitation at 256 points on both spans was used to compute the model distributions. The lowest natural mode at 11·79 Hz was the in-phase mode shown in Figure 9(a), and the second natural mode at 12·58 Hz was the out-of-phase mode in Figure 9(b). These results are in accord with expectations from the previous discussion.

5. CLOSING REMARKS

Investigation of vibration in the principal span of a continuous band system requires consideration of the secondary span and wheel responses in the modeling. In spans with vanishing equilibrium curvature, the vibration of the principal and secondary spans decouple. A finite equilibrium curvature of the spans is the key to the coupling and to the splitting of the degenerate natural frequencies associated with the identical spans.

Damping of the secondary span vibration simultaneously dampens response in the principal span when the responses are coupled. Because the secondary span is often more accessible for vibration control than the principal span, an important opportunity exists for active and passive vibration control of the principal span through excitation or damping of the secondary one.

REFERENCES

1. C. D. MOTE JR. 1972 *Shock and Vibration Digest* **4**, 2-11. Dynamic stability of axially moving materials.
2. A. G. ULSOY, C. D. MOTE JR. and R. SZYMANI 1978 *Holz als Roh-und Werkstoff* **36**, 273-280. Principal developments in band saw vibration and stability research.
3. C. D. MOTE JR., G. S. SCHAJER and W. Z. WU 1982 *Shock and Vibration Digest* **14**, 19-25. Band saw and circular saw vibration and stability.
4. C. D. MOTE JR. 1965 *Journal of the Franklin Institute* **279**, 430-444. A study of bandsaw vibrations.
5. D. W. ALSPAUGH 1967 *Journal of the Franklin Institute* **283**, 328-338. Torsional vibration of a moving band.
6. A. G. ULSOY and C. D. MOTE JR. 1982 *Transactions of the American Society of Mechanical Engineers, Journal of Engineering for Industry* **104**, 71-78. Vibration of wide band saw blades.
7. C. D. MOTE JR. 1968 *International Journal of Mechanical Science* **10**, 281-295. Divergence buckling of an edge-loaded axially moving band.
8. R. O. FOSCHI and A. W. PORTER 1970 *Canadian Western Forest Products Laboratories Report No. VP-X*-68. Lateral and edge stability of high strain bandsaws.
9. G. PAHLITZSCH and K. PUTTKAMMER 1974 *Holz als Roh-und Werkstoff* **32**, 52-57. Beurteilungskriterien für die Ausklenkungen von Bandsageblattern.
10. A. M. GARLICKI and S. MIRZA 1978 *Fourth Symposium, Engineering Application of Solid Mechanics, Ontario Research Foundation* **2**, 273-287. Lateral stability of wide band saws.
11. C. D. MOTE JR. 1968 *Journal of the Franklin Institute* **285**, 329-346. Dynamic stability of an axially moving band.
12. A. L. THURMAN and C. D. MOTE JR. 1969 *Journal of Applied Mechanics* **36**, 83-91. Free periodic nonlinear oscillation of an axially moving strip.

APPENDIX: LIST OF SYMBOLS

E_p, E_s	energies of the principal and the secondary spans of the band
EI	uniform bending stiffness
l	length of each span
M	bending moment
R	radius of curvature of the wheel
T	band tension
Y_p, Y_s	transverse displacements of the principal and the secondary spans of the band
ρ	density of the band
ω_i, ω_0	natural frequencies of the lowest "in-phase" and "out-of-phase" vibration modes of the band respectively
ω_{ave}	average frequency $\frac{1}{2}(\omega_0+\omega_i)$
ω_{mod}	modulation frequency $\frac{1}{2}(\omega_0-\omega_i)$